# Chapter V
# Calibration and Measurement of Signal Strength for Sensor Localization

**Neal Patwari**
*University of Utah, USA*

**Piyush Agrawal**
*University of Utah, USA*

## ABSTRACT

*A number of practical issues are involved in the use of measured received signal strength (RSS) for purposes of localization. This chapter focuses on device effects and modeling problems which are not well covered in the literature, such as transceiver device manufacturing variations, battery effects on transmit power, nonlinearities in RSSI circuits, and path loss model parameter estimation. The authors discuss both the negative impacts of these effects and inaccuracies, and adaptations used by particular localization algorithms to be robust to them, without discussing any algorithm in detail. The authors present measurement methodologies to characterize these effects for wireless sensor nodes, and report the results from several calibration experiments to quantify each discussed effect and modeling issue.*

## INTRODUCTION

Signal-strength based localization can be deceptively simple. Receivers are generally capable of measuring and reporting to higher layers information about received signal strength, so it can seem like it should be easy to take these measurements and use them directly in a localization algorithm. Significant research has developed algorithms for localization, assuming that measured signal strength has already been converted into distance estimates, and little research discusses the details of how to perform those conversions.

Copyright © 2009, IGI Global, distributing in print or electronic forms without written permission of IGI Global is prohibited.

Multipath fading in radio channels is universally regarded to be the main degradation to RSS-based location estimates, and rightfully so – significant shadowing and small-scale fading caused by the channel is largely unavoidable and unpredictable. Beyond that, however, there can be severe degradations caused by a lack of understanding of the non-idealities of the measurement process, and inaccurate knowledge of channel parameters. If RSS-based localization is to be attempted, a designer must be able to characterize and cope with these non-idealities and imperfect knowledge.

This chapter is written to present real-world calibration and non-linearity problems in RSS measurements and how to deal with them. We follow RSS-based localization from the transmitter to the receiver, and in multiple stages in the receiver, as shown in Figure 1. The intended audience is anyone who intends to implement or has already implemented RSS-based localization algorithms which are to operate well in real-world deployments. We present our work in RSS-based localization algorithms only briefly. We have found that the experience of accurately using measured signal strength, in general, is as challenging as the localization algorithm itself.

Our chapter is organized as follows. First, in section PROPAGATION EFFECTS, we relate some of the literature on path loss models as a function of distance and the effects of shadowing and multipath fading. Then, in section DEVICE EFFECTS, we discuss a method for accurately characterizing transmit power as a function of device settings and battery voltage, and receiver RSSI values as a function of the particular device performing the measurement. The transmit power characteristics are necessary to translate measured RSS into accurate path loss values. The receiver characterization reveals the details of the nonlinearities in measured RSSI. Then, section CHANNEL EXPERIMENTS WITH POWER CONTROL describes a protocol and algorithm for transmit power control, to avoid RSSI saturation without sacrificing node connectivity. Thirdly, the section titled RANGING USING MEASURED PATH LOSS discusses the conversion of path loss, calculated using the results of the DEVICE EFFECTS section, into an estimate of range. Finally, a section called RSS-BASED LOCALIZATION ALGORITHMS discusses how the lessons discussed in this chapter apply in our RSS-based location algorithm implementation.

*Figure 1. RSS-based localization requires characterization of both the transmitter and receiver, and the ability to convert measured RSSI into path loss prior to input into a localization algorithm. Path loss estimation requires knowing transmitter parameters and may require feedback to the transmitter to control its transmit power.*

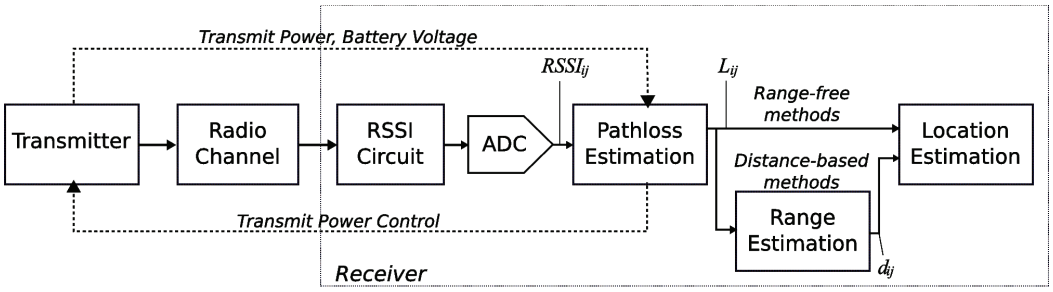

## PROPAGATION EFFECTS

Multipath fading, shadowing, and antenna effects cause great variations in the measured RSS in real-world environments, degrading its ability to produce accurate distance or position estimates. This section serves to emphasize these well-reported effects in order to position the importance of studying device effects on measured RSS. As we delve deeper into device effects which cause RSS errors, we will be able to position them in context to the larger problem of RSS-based position estimation.

Path losses, on average, increase with distance – the increase is due to "large-scale" path loss (Hashemi, 1993), which are proportional to $10n_p \log_{10} d$, where $n_p$ is a path loss exponent, and d is the path length. But the path loss between two radios at particular positions is very much a function of the objects in the environment between them and the position and orientation of the antennas. Movement on the order of centimeters or changing channel from one frequency to another can cause dramatic path loss differences because of "multipath fading" or "small-scale fading".

Indoor environment propagation effects are particularly a problem for localization. As defined in Pahlavan, Li, and Makela (2002), when the line-of-sight path arrives with more power than any other multipath, it is called a dominant line-of-sight (DLOS) link. In indoor environments, only receivers in a small area around the transmitter are found to be likely to be DLOS. Most areas indoors have an LOS path shadowed by walls and objects; this shadowing decreases the received power, and the RSS becomes dominated mostly by multipath power from many different directions. Besides being impacted by shadowing, these situations are more strongly affected by small-scale fading because many multipath signals contribute to the received signal. When more multipath signals arrive from more directions, the statistics of small-scale fading change from Ricean to Raleigh and thus become more severe (Rappaport, 1996). Further, as we will discuss in more detail in the "Distance Estimation Equations" section, the errors in distance estimates are multiplicative; thus are more severe at longer path lengths. In short, the fading problems increase as the distance between the transmitter and receiver increases.

It is important to note that shadowing is not solely a degradation for RSS-based localization systems. RSS fingerprinting algorithms (as described in the "RF Fingerprinting Algorithms" section) take advantage of the fact that shadow fading is a feature-rich, spatially-correlated random field which is mostly stationary over time. By recording this field and using it to match measurements to a location, RF fingerprint-based algorithms exploit location-specific shadowing variations to benefit localization. In such systems, it is only small-scale fading and the change in shadow fading which degrade localization algorithms.

Errors in RSS measurements also come from the fact that real-world antennas have directionality and the orientation of a node is not known a priori. This is exacerbated by objects to which devices are attached – anything metal or mostly water (people) would block RF propogation in its direction, attenuating the signal by as much as 15 dB. King et. al. (2006) have found that these antenna orientation issues are important to measure in calibration of RSS fingerprint-based localization systems, as will be discussed in the "RF Fingerprinting Algorithms" section. Generally, multipath arrive at a receiver from many directions, and the measured RSS will depend on the powers of the multipath which arrive in the same direction as the directionality of the antenna. Algorithms such as King et. al. (2006) actually use the antenna directionality to estimate the device orientation in addition to its position.

## DEVICE EFFECTS

Simple wireless devices can measure and report a quantized measurement of the received signal strength (RSS) of a received packet. This measurement of RSS is typically referred to as the received signal strength indicator (RSSI). For localization purposes, we actually require the path loss, that is, the actual dB loss experienced between transmitter and receiver antennas, which is related to distance between the two antennas. It is not trivial to convert RSSI into path loss. In this section, we show how wireless nodes can be calibrated so that RSSI measurements can be converted into path losses.

Path loss $L_{ij}$, in dB, on a link between transmitter j and receiver i is defined here to be the difference between the dBm transmit power $P_T$ and the dBm received power $P_R$,

$$L_{ij} = P_T - P_R$$

In this section, we detail how transmit power and received power are functions of the device characteristics, parameter settings, and battery voltage.

This section does not propose that all nodes should be characterized and calibrated for purposes of system deployment. However, it is often important to calibrate one set of nodes for research and development purposes. It is critical to know how much devices vary and thus how much is lost when devices are not calibrated, even if we have no intention of deploying systems of calibrated nodes.

We intend to characterize two device characteristics that make measured RSSI vary:

- Transmit power device variations
- Transmit power battery variations
- Receiver RSSI circuit device variations

We show calibration measurements for the Crossbow Mica2 sensor in this chapter, but other wireless sensor modules can also be calibrated using this basic procedure.

### Transmit Power Device Variations

Typically, the transmit power of a radio IC can be set among a discrete set of possible power levels. For wireless sensors, the need to conserve energy makes this a key requirement for the radio IC. When nodes are communicating at short range, it will conserve energy to transmit at a lower power. In addition, in interference-limited networks, reducing transmit power to the minimum required level helps reduce interference and allow higher communications rates. When nodes are transmitting at different power levels, it will be critical to know exactly what transmit power is being sent so that path loss $L_{ij}$ (above) can be computed. And, as we will show, transmit powers may vary from device to device even for the same nominal "power level" and battery voltage, due to manufacturing variations.

Transmit power differences between nodes are to blame for many of the asymmetric links in sensor networks, that is, when node i can be received at node j, but node j cannot be received at node i. Extensive analysis is reported by Zuniga and Krishnamachari (2007). Similar to the communications case, an asymmetric link can cause difficulties for a sensor localization algorithm. Some localization algorithms would not collect data on an asymmetric links because of the lack of a bidirectional communications link – data collection and exchange protocols could fail on that link. Zuniga and Krishnamachari (2007)

report a variance of transmit power of 6 $(dB)^2$. This variation includes the effects of battery variations and device variations.

To provide a controlled measurement-based quantification of transmit power variation, we present measurements of a set of Crossbow Mica2 nodes, which use the TI/ChipCon CC1000 radio IC. Our calibration experiment is shown in the block diagram in Figure 2. The calibration procedure can be described in the following steps:

- Each node is powered from a variable DC power supply set to 3.0 V so that we can study the transmit power variation separately from battery variation.
- Each node is programmed to periodically transmit data packets at a specified transmit power code.
- A node is RF shielded by placing it in an aluminum box, and its RF output port is connected via RF/coaxial cable to a spectrum analyzer (Agilent E4405B) in peak power mode, as shown in Figure 2.
- While connected, the transmit power code of the node is changed from one to the next and the measured transmit power is recorded for each.

Table 1 reports the transmit power values (in dB) for the different transmit power codes for the particular device under test. In the experimental process, we kept the transmit frequency at 903 MHz.

We have characterized multiple transmitters in order to consider the variations between devices. The transmit power calibration values for sixteen different Mica2 nodes are plotted in Figure 3 as a function of transmit power code. There is noticeably higher variance in transmitted power between devices at low transmit powers. The largest variation is at the lowest transmit power level, for which transmit power varies from -29.1 dBm to -32.7 dBm, a difference of 3.6 dB. But, over all transmit power levels, the standard deviation of the transmit power ranges from 0.15 to 0.91 dB, for an overall RMS standard deviation of 0.45 dB. On the whole, we have that the difference between the average and the actual transmit power for a given device is random with standard deviation 0.45 dB.

## Transmit Power Variation with Battery Voltage

However, this is the device variation, without considering the battery voltage. As time passes, the battery power is drained, and the voltage produced by the battery reduces. At some point, when the battery voltage becomes too low, the sensor, or the radio will fail. But before failure, changes in battery voltage

*Figure 2. Block diagram for transmitter calibration*

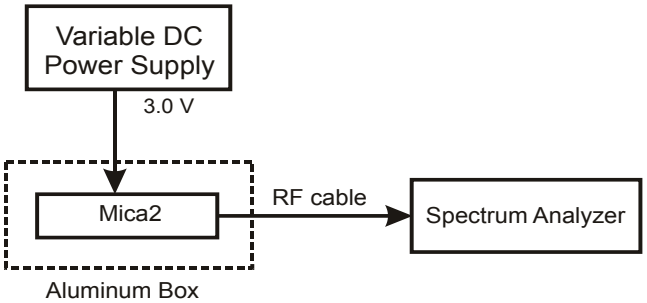

*Table 1. Transmit power vs. transmit power code for Mica2 device under test*

| Power Code (hex) | Output Power (dBm) | Power Code (hex) | Output Power (dBm) | Power Code (hex) | Output Power (dBm) |
|---|---|---|---|---|---|
| **0x02** | -31.00 | **0x0B** | -14.71 | **0x70** | -5.23 |
| **0x03** | -26.56 | **0x0C** | -13.30 | **0x80** | -3.94 |
| **0x04** | -23.84 | **0x0D** | -12.64 | **0x90** | -3.09 |
| **0x05** | -21.56 | **0x0F** | -11.22 | **0xB0** | -1.42 |
| **0x06** | -19.92 | **0x40** | -9.99 | **0xC0** | -0.94 |
| **0x07** | -18.33 | **0x50** | -8.08 | **0xF0** | -0.37 |
| **0x08** | -16.97 | **0x60** | -6.49 | **0xFF** | -0.03 |
| **0x09** | -15.94 | | | | |

*Figure 3. Transmit power in dB vs. transmit power code for 16 different Mica2 devices*

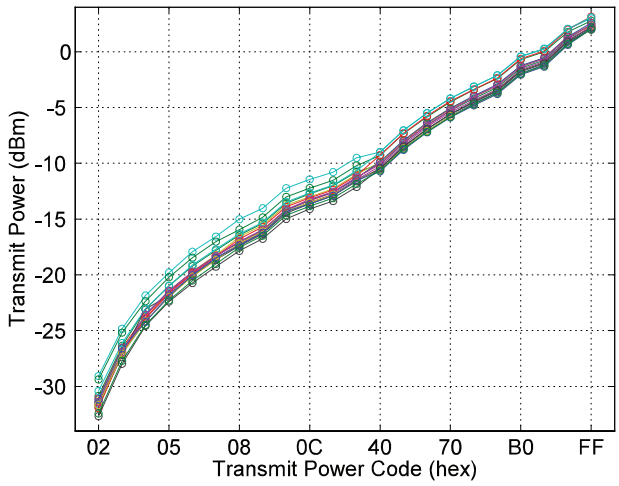


affect the transmitted power. In fact, the power that a transmit amplifier can produce is proportional to the square of the battery voltage. An amplifier has an efficiency, which relates to how much of the battery power can be converted to RF transmit power. In general, we can consider the transmit power, $P_T$, as a function of battery voltage $V_{batt}$,

$$P_T(V_{batt}) = P_T(V_0) + \alpha 20 \log_{10}(V_{batt}/V_0) \quad (1)$$

where $P_T(V_0)$ is the transmit power measured at a reference voltage, $V_0$, and $\alpha$ is an efficiency constant. For our measurements, we used a reference voltage of $V_0 = 3.0$ Volts.

To characterize the transmit power as a function of battery voltage, we tested multiple Mica2 nodes using a modification of the test procedure shown Figure 2, in which we changed the DC voltage provided by the variable DC power supply in the range of about 2.4 to 3.3 Volts. At each tested DC voltage, we recorded the transmit power on the spectrum analyzer. The results are shown in Figure 4 for two of the nodes. For the linear model above, the value of $\alpha$ is calculated to be 0.67. This value is

*Figure 4. Transmit power in dBm as a function of the battery voltage. The solid line indicates the best fit to the linear model, with* $\alpha = 0.67$.

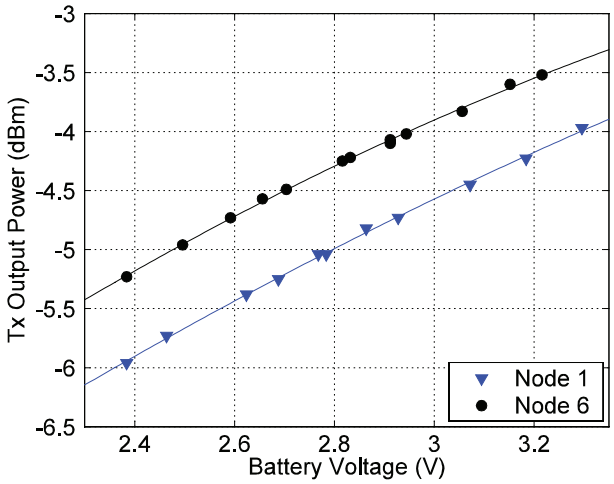


largely constant across nodes. So, while the value of $P_T(V_0)$ is not the same between nodes, the slope of the transmit power as a function of battery voltage near 3.0 Volts may be approximated as identical between nodes.

## Discussion

Since devices do vary, even with identical devices, it is clear that in a large-scale sensor localization system, device transmit powers will differ from their stated, nominal, values. An important question is, how are localization algorithms affected by these random transmit power variations? In the "Non-parametric Localization Algorithms" section, we discuss one type of algorithm which can be robust to transmit power variations, due to its use of RSS differences.

We also mention existing analytical analysis reported by Patwari and Hero (2006) which reports the Bayesian Cramèr-Rao bound (CRB) on coordinate estimator variance when the transmit powers are random. The bound provided by the Bayesian CRB is useful because it is independent of algorithm; any estimator will have root mean-squared error (RMSE) greater than its bound. In this analysis, the transmit powers of each device was assumed to be random, and Gaussian, with a given standard deviation. The increase of the bound is reported to describe the performance degradation caused by not knowing the exact transmit power. From the example numerical results, for a standard deviation of transmit power of 1 dB, the bound on RMSE increases by 1-3% (depending on the setup). However, a key finding of the bound analysis is that the two bi-directional measurements on a link (both $L_{ij}$ and $L_{ji}$) must both be used in the localization algorithm; it is not sufficient to average the two together, $\frac{1}{2}(L_{ij} + L_{ji})$, and use only that average. When using only the link bi-directional average, an algorithm is no longer able to adaptively estimate node transmit powers, and the RMSE bound increases much more dramatically, as much as 25% when the standard deviation of transmit power is 5 dB. In sum, the impact of transmit power variations can be severe, but only when the standard deviation of transmit power is high. Algorithms could be designed to adaptively estimate each node's deviation from its nominal transmit power

and then adjust the coordinate estimate as a result. For example, use the difference values, $L_{ij} - L_{ji}$, for all j, to estimate the deviation of the transmit power of node i from its nominal value.

## Receiver RSSI Circuit Device Variations

Assuming that calibrations described in past two sections are complete, we know very accurately the transmit power of a calibrated node, given its transmit power code and battery voltage. Now, we can proceed to use a fully characterized transmitter to calibrate a receiver's RSSI characteristic. This process will allow us to accurately translate the measured RSSI in Volts to the actual path loss in the channel.

We show in this section that wireless sensors report an RSSI which has a non-linear relationship with received power. For some range of RSSI, we can make a linear approximation, but we then must be careful when using signal strength measurements that the receiver is operating in a linear region of RSSI. In this section, we report characterization of the Crossbow Mica2 mote, which uses the CC1000 radio IC, but we have also observed the non-linear characteristic on the Crossbow TelosB mote (with a CC2420). We believe that, in general, inexpensive radios are not designed to achieve linear measurements of received power, because communications applications generally do not require it.

In our measurements, we input a known received power in dBm into a device and record the RSSI value in Volts. We do this using the experimental setup in Figure 5, designed to provide a known received power, and to remove the effects of RF leakage. The mote 1 in Figure 5 is placed in a RF shielded box and programmed to transmit with known transmit power code (0x0F) and known battery voltage (3.0V) from a power supply. From the results presented already, we know that this node transmits -11.22 dBm with these settings (from Table 1). We choose from among several SMA-connectorized attenuators, with a range of attenuation values, to achieve the desired link loss. Inside a second shielded box we place mote 2, which has the receiver under test, and is connected to the output of the attenuators via an SMA to MMCX cable. A third Mica2 node is programmed to receive the measured data from mote 2 and to communicate it to a laptop.

Figure 6 shows the recorded RSSI values from the experiment for a wide range of received power values. The results show two critical lessons for the use of measured signal strength:

- **At high received power (-50 dBm and above) the RSSI values saturate**, and do not have a linear relationship with the actual received power. Although it is very possible for two proximate

*Figure 5. Block diagram for receiver calibration*

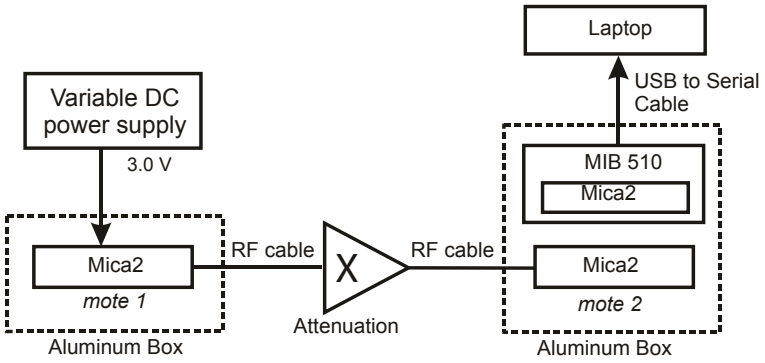

nodes to record a received power at or above -50 dBm, it is not useful for the purpose of accurately measuring link path loss.

- **At power levels below -90 dBm, packets are not correctly demodulated**. Thus path loss integers are not reported for received power levels below -90 dBm. However, we note that in the above calibration setup, if RF shielding is not done properly, and RF power leakage is allowed to circumvent the attenuators (possibly from poorly connected, or low quality cables), you would receive packets, and for this node, the RSSI would be around 0.85 V. If a second non-linear region exists at the bottom right (at low received power) of Figure 6, then it is likely that RF leakage is the problem.

For the values in the linear range (-50 to -90 dBm) we calculate a linear fit. This linear fit for this node's receiver is given by

$$P_R(RSSI) = -50.6RSSI - 44.36 \text{ [dBm]} \quad (2)$$

where RSSI is the path loss integer reported by the receiver, and $P_R$ is the actual received power. This measured result is slightly different from the result listed on the CC1000 data sheet, which had reported that the $P_R = -51.3$ RSSI – 49.2 in dBm (as cited in Whitehouse, Karlof, and Culler, 2007). We do not know how the data sheet formula was determined, so our best guess regarding the 5-6 dB offset is that it is due to RF front end differences prior to the CC1000 radio IC in the tested device (the Mica2) compared to the device used in the CC1000 manufacturer calibration tests.

We note also that other research has been conducted to characterize receiver differences for communications applications. Zuniga and Krishnamachari (2007) also included characterization of receiver noise floor. The analysis uses the noise floor power value in order to determine whether or not a packet received at a given power can be demodulated or not. Such a model only requires one parameter, the noise floor, while our analysis for localization purposes must characterize the function of received

*Figure 6. Measured RSSI value vs. actual received power for a tested Mica2 node, and a linear fit for the data points which do not experience saturation*

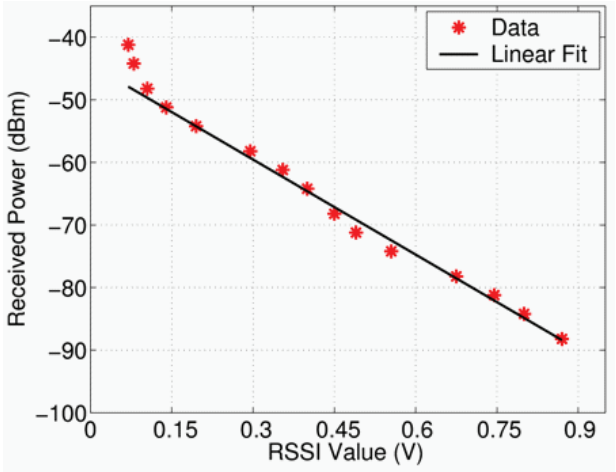

power vs. RSSI value. Zuniga and Krishnamachari (2007) find that this receiver noise floor value has a variance of 3 $(dB)^2$.

In the "linear" region of the measured characteristic of Figure 6, there is some small non-linearity in the Mica2 RSSI characteristic. The actual received power in the 0.25 V < RSSI < 0.35 V range is slightly higher than the linear fit, while the actual received power in the 0.45 V < RSSI < 0.6 V range is slightly lower than the linear fit. We find this consistent across Mica2 nodes. We believe this is specific to the Mica2 implementation, but that other radio ICs will also see small non-linearities. The standard deviation of error in the linear fit, for the data recorded in the linear region, is about 1.1 dB.

## Discussion

Point (1.) above deserves extra emphasis, because it indicates a key requirement for use of signal strength between nearby nodes. Intuitively, one might expect that recorded RSSI is most accurate when there are short distances between nodes. However, this is not true if the nodes are transmitting at high power levels. In fact, if nodes are to be deployed densely, nodes must turn down their transmit power! This is counter-intuitive, since lower transmit power results in lower signal to noise ratio, and shorter range. However, for purposes of path loss measurement and path loss-based ranging, very high received powers saturate the receiver and make the measured RSSI uninformative.

Nodes should not turn down their power at the expense of node connectivity. The large-scale experiments in Whitehouse, Karlof, and Culler (2007) show that localization performance degrades quickly when the connectivity degrades. By lowering the transmit power or by lowering the antennas closer to the ground (which increases path losses) the experiments reduce connectivity and show that an algorithm's ability to localize is quickly lost.

Point (2.) also is critical to understand why observed received powers are sometimes higher than predicted by a path loss model at long distances. This saturation is a "observation bias": we can only measure received power if it is above a threshold (about -90 dBm in Figure 6). Assume that at a given distance, our best propagation model says that the average received power should be below the threshold. But we can only measure received powers above the threshold. Thus when we report an average experimental received power for nodes separated by that distance, it will be above the threshold. This effect introduces bias into localization algorithms (Costa, Patwari, and Hero, 2006).

## Summary

We have used calibration in two ways: to enable high accuracy path loss measurements, and to quantify the errors caused by uncalibrated nodes. Transmitter power outputs variations have a standard deviation from 0.15 to 0.91 dB at the highest and lowest transmit power level, respectively. Transmit power levels change about 1 dB between new batteries to dead batteries. Receiver RSSI can be used to indicate received power, and as long as the RSSI is in the linear region, we can expect it to contribute 1 dB of standard deviation to our measurement. In total, since variances add, the overall standard deviation of error due to device non-characterization could be as little as 1.4 to 1.7 dB. This, again, assumes that the average device characteristic is well known, and that receivers are operating in the linear region.

This standard deviation of error may have minimal impact on some common applications. For example, for ranging, the multipath fading and shadowing variances will far outweigh this non-characterization error variance. Thus we do not suggest device calibration as a necessary procedure for all applications. However, we must ensure that received powers are not in the saturation range of the receiver.

## CHANNEL EXPERIMENTS WITH POWER CONTROL

One main lesson learned from the device calibration work is that accurate RSS-based ranging and localization should take place when the received power does not reach either of two extremes. The received power must be high enough to demodulate packets, but not so high power as to place them in their saturation region. In the first extreme, if the RSSI of all neighbors' packets are measured to below about .13 V, it will be very difficult to distinguish the actual received power (in particular when device variations are taken into account), and all neighbors will seem equally close to the receiver. At the other extreme, if neighbors' packets arrive with power near or below the receiver threshold, then we are missing packets from neighbors, and we will not do as good of a job in localization as we could.

To some extent, these problems can be controlled by changing the transmit power. The Mica2 node has a transmit power range of about 30 dB, and in general, wireless sensors have the ability to change their transmit power over a wide range. By lowering the transmit power to its minimum it is possible to completely avoid the first extreme, in which received powers are too high. We have run many localization experiments with a node density of 10-20 nodes per square meter with the transmit power set to its lowest power setting, and see good results from our RSS-based localization algorithm, described in Patwari, Agrawal, and Hero (2006). However, when transmit powers are set higher, measured RSSI values are nearly identical, regardless of path length. In the second extreme, with the transmit power set to its highest, we can run localization experiments with long distances of 10-20 m between nodes, as long as each node is within communication range of a few other nodes.

However, we cannot limit WSN localization to situations in which local node densities are well known prior to deployment. In this section, we introduce a simple closed-loop power control protocol and algorithm to automatically avoid the two extremes of low and high received powers.

### Protocol

In order to obtain feedback regarding its transmit power, a node must learn from its neighbors. Given that node i can communicate with K nodes, $j_1, j_2, \ldots, j_K$, we denote the neighbor set of node i as $H_i = \{ j_1, j_2, \ldots, j_K \}$. In this power control protocol, node i transmits feedback to each node $j \in H_i$ regarding the RSSI node i measured during reception of packets from j. We denote this as $RSSI_{ji}$, and it is the measured RSSI at node i for the packet transmitted by node j. With this notation, the "power control packet" transmitted by node i has contents shown in Figure 7.

Each node, each round, transmits one power control packet to provide feedback to its K nearest neighbors regarding its measured RSSI values. In our experiments, we use K = 12.

*Figure 7. Power control packet transmitted by node i*

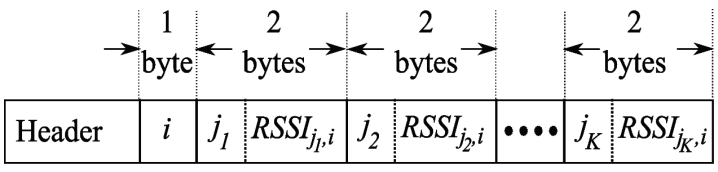

## Algorithm

When node i receives any power control packet, it searches in the list of j's neighbors, $i_1, i_2, \ldots, i_K$, to find its own node number. If i is a neighbor of j, then it records $RSSI_{j,i}$ as an "incoming RSSI" from node j. It must collect each incoming RSSI value from the power control packet of one of its neighbors. To aggregate them, node i then averages all RSSI values on record to calculate its mean incoming RSSI. This value summarizes the feedback received from all of its neighbors.

The decision about the transmit power, in this algorithm, is solely a threshold test on the mean incoming RSSI. We have two rules:

- If the mean incoming RSSI is less than 0.25 V, reduce the transmit power.
- If the mean incoming RSSI is greater than 0.6 V, increase the transmit power.

The transmit power is raised or lowered by one transmit power code at a time. Note that at low or very high RSSI, we cannot predict how changing the transmit power code will impact the mean incoming RSSI, because of the nonlinear effects of either RSSI saturation or nodes being out-of-range. Thus we do not believe that an optimal transmit power can be directly computed.

## Results

We implemented the above transmit power control algorithm and ran it to show that the above simple algorithm is able to adapt the transmit powers in a sensor network to an appropriate level. In an experiment, we program a group of 16 nodes to run the power control algorithm described above. This program initializes at a transmit power code 0x0F, which from Table 1, corresponds to a transmit power of -11 dBm. Then, we place the 16 nodes on a carpeted floor in a 2 m by 2 m square area. These nodes are at a high density, so many of the received powers are initially higher than -50 dBm, within the non-linear RSSI region we wish to avoid. Clearly, the transmit powers should be reduced.

We watch how the sensors respond and change their transmit power code at each iteration, or "sequence number", of the algorithm. Nodes transmit packets with a sequence number which is incremented after each transmission. Note also that nodes use a slow frequency hopping, so the frequency changes with

*Figure 8. (a) Transmit power code and (b) mean incoming RSSI vs. sequence number, recorded by nodes one and two during the power control experiment*

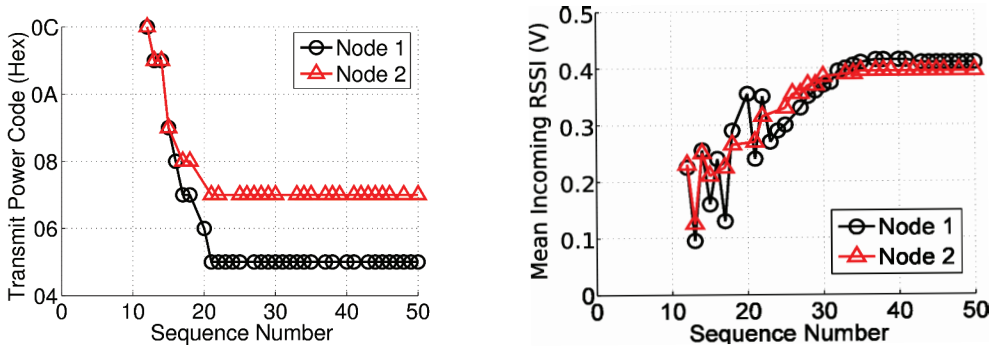

each transmission. Our base unit does not synchronize fast enough to receive packets in the first few sequence numbers. First, we observe in Figure 8(b) how the mean incoming RSSI value is initially as low as 0.1 V. While this value is below 0.25 V, the transmit power decrements each sequence number. The mean incoming RSSI is noisy during this time, because it is re-initialized each time the transmit power is changed. During each time period, it may hear from a large number of neighbors, but since packet reception rates are approximately in the 70-80% range, we will hear from a random subset each time, which leads to a large variation in the mean incoming RSSI over time. There is also a noticeable delay in the control loop, which leads to the asymptotic mean incoming RSSI approaching a value around 0.4 V, rather than the threshold of 0.25 V. This is due to the latency introduced by frequency hopping.

### Summary

One major difficulty with RSS-based ranging is the nonlinear effect at close range, and the lack of connectivity at low node densities. Instead of a constant transmit power, we use an adaptive power control algorithm to set the transmit power to an acceptable value. Assuming that we have performed the transmit calibration procedure (discussed in the earlier section) on a few of the nodes, we will be able to program the nodes to compute path loss from the RSSI and the known transmit powers of its neighbors.

## RANGE-FREE LOCALIZATION FROM MEASURED PATH LOSS

Up until this point, we have only talked about accurately computing measured path losses on links. Much of the sensor network localization algorithm literature deals with range-based localization algorithms, which require converting path loss measurements into a distance estimate prior to estimating the node coordinates. However, there is a significant interest in localization without such conversion; these "range-free" algorithms can provide useful characteristics compared to range-based localization.

In this section, we discuss three types of algorithms which do not require distance estimates. These three types are:

- Connectivity-based localization
- Non-parametric RSS-based localization
- RF fingerprint-based localization

### Connectivity-Based Localization

Localization methods which use only whether or not two nodes can communicate are called proximity or connectivity-based methods. Connectivity is effectively a binary quantization of the received power, since digital communications receivers are largely unable to receive packets when the received power is below a receiver threshold. Thus two nodes are either "in-range" or "out-of-range". The threshold between the two may be the actual physical limits of the radio, or may be set to some other pre-determined RSSI value. Range-free algorithms are excellent low-maintenance and low-setup cost localization systems for applications where the highest accuracy is not required. In some applications, knowing that a receiver is in-range of one or more known-location transmitters is more than enough location information. Several algorithms have been proposed for use with connectivity, including Bu-

lusu, Heidemann, and Estrin (2000), and Niculescu and Nath (2001). They range from simply finding the centroid of the coordinates of in-range nodes (Bulusu et. al., 2000) to using the shortest-path hop count as a distance metric (Niculescu and Nath, 2001).

The main problem with range-free localization is that quite a bit of information is lost by quantizing the RSSI into one bit. In our theoretical analysis, we found that we should expect at least a 50% increase in standard deviation of localization error compared to using unquantized RSSI values, even if the threshold is set optimally (Patwari and Hero, 2003).

## Non-Parametric Localization Algorithms

Non-parametric RSS-based localization algorithms directly use RSSI measurements. Ecolocation (Yedavalli, Krishnamachari, Ravulla, and Srinivasan, 2005) and ROCRSSI (Liu, Wu, and He 2004) are algorithms which use the order information of the path loss values at node i, when the path loss values are sorted from smallest to largest. Then, these algorithms constrain the distance between node i and its closest neighbor to be less than the distance to its 2$^{nd}$ closest neighbor, which must be less than the distance to its 3$^{rd}$ closest neighbor, and so on. These constraints graphically imply concentric circles, for the closest to the furthest neighbor. The Ecolocation algorithm finds a region for each sensor which best meets the simultaneous constraints imposed by all the neighbor distance orderings. However, the full solution can be computationally complex because of the large number of simultaneous constraints, and is a centralized algorithm. The APIT method of He, Huang, Blum, Stankovic, and Abdelzahar (2003) similarly reduces the area of possible location, in its case, by testing each set of three nodes to see whether the device-to-be-located is within, or outside of, the triangular area formed by the three nodes. The APIT triangle test requires only a comparison of path loss measurements between neighboring nodes, but it assumes a relatively high density of anchor nodes (or anchor nodes with high transmit power) compared to the APS method of Niculescu and Nath (2001).

## RF Fingerprinting Algorithms

In RF fingerprint-based algorithms, the RSS between a node and many fixed access points are recorded, and used together as a vector "fingerprint" of the location of the node (King et. al., 2006, and Bahl and Padmanabhan, 2000). This method, prior to deployment, takes thorough measurements of the fingerprint of a test node moved to every possible location in the area of deployment (e.g., in a building), and possibly facing each direction at that location. At each location and facing direction, the fingerprint of the test node is recorded and stored in a database. The localization algorithm, once deployed, simply searches for the closest measurement in the database – that measurement's location is estimated to be the current node location. This notion of "closest" is a function of the measured RSSI values (e.g., Euclidean distance between RSSI vectors in Bahl and Padmanabhan (2000)). The chosen distance metric may be optimal for certain statistical error model (e.g., the Euclidean distance metric for Gaussian errors), so an RF fingerprinting algorithm makes an implicit assumption about the statistical model for path loss measurements. The RF fingerprinting algorithm does avoid significant other modeling requirements of distance-based localization algorithms.

Clearly, RF fingerprinting methods require a huge investment of time prior to deployment, and a large fixed infrastructure – two requirements not typically present for environmental wireless sensor networks. However, for sensor systems which operate in buildings where other WiFi backbones exist,

RF fingerprinting methods can provide a high-accuracy, large scale localization system. RF fingerprinting methods have been commercialized for the active RFID / real-time location systems (RTLS) market segment, and companies such as Ekahau, Inc. and AeroScout, Inc. deploy such systems. As time passes and the arrangement of a building interior changes (e.g., every 3 months), such systems require re-measurement of the fingerprint database to keep accuracy high. Current research efforts show promise in the reduction of measurement requirements to build the database, for example, as in Fang, Lin, and Lin (2008).

### Discussion

These three types of range-free algorithms require only relative notions of path loss, and thus do not require a conversion to distance. In all methods, measured RSSI is either compared to a threshold or to other RSSI measurements. When all nodes transmit at identical power levels, the RSSI can be used directly. But when transmit powers differ, either purposefully due to power control or simply due to device variations, RSSI should be converted to path loss to see the full benefits of the proposed non-parametric localization algorithms.

Non-parametric localization algorithms do eliminate the need to estimate distance from path loss. As will be discussed in the following sections, distance estimation requires additional knowledge of environmental propagation characteristics, which can be difficult to accurately provide to a general-purpose localization system.

## RANGE-BASED LOCALIZATION FROM MEASURED PATH LOSS

Despite advances in "range-free" algorithms, there is often a need to use a distance-based location algorithms. When sensor networks are deployed where little infrastructure exists, and thus RF fingerprinting approaches will not work, there are often benefits to having an explicit range estimate in localization algorithms. For distributed wireless sensor network localization, there are many examples of range-based localization algorithms in the literature.

Another argument for including range estimation is that, while there is a clear delineation in the literature between range-based and range-free algorithms, practical deployed localization systems will often benefit from using a mix of both types of algorithms. For example, range-free localization algorithms may gain from the use of range estimates as a consistency check. Similarly, range-based algorithms will likely need a method for online local determination of propagation and device parameters, which at one extreme, is no different than non-parametric localization approaches.

In this section, we present a discussion of the conversion of path loss to distance between two nodes. This conversion requires models for path loss, which is not only a function of distance, but many other environmental and propagation effects. We first present these distance and noise models, and then present information about estimators of distance given measured path loss.

### Exponential Decay Model

The most common model for the ensemble mean of path loss at a particular distance between transmitter and receiver is that path loss is linearly proportional to the logarithm of that distance (Rappaport, 1996, and Hashemi, 1993). This proportionality is typically written as follows:

$$E[L_{ij}] = L_0 + 10n_p \log_{10} \frac{d_{ij}}{d_0} \quad (3)$$

where $L_0$ is the path loss at a reference distance $d_0$, and $n_p$ is called the path loss exponent, and the $E[L_{ij}]$ indicates the expected value. Here, path loss is expressed in dB, which is 10 times the log base 10 of the linear multiplicative channel loss. The values of $L_0$ and $n_p$ are dependent on the environment in which the sensors are deployed.

The model of (3) assumes no site-specific knowledge. In situations where we know the positions of the two nodes and the environmental obstructions in between them (interior or exterior walls, floor losses, trees, buildings, etc.), we could estimate the mean loss much more accurately. For example, Durgin, Rappaport, and Xu (1998) models each type of obstruction in the path as an attenuator with a constant loss, and estimates these constants from a set of measurements. For the purposes of localization in WSN, site-specific information may be limited. When it is available, it introduces sharp discontinuities in the path loss as a function of the two node coordinates, making optimization-based algorithms fail. However, such models have made impact in RSS fingerprint-based localization by allowing fingerprint measurements to be interpolated, and thus requiring much less dense manual measurements (Zhu, 2006).

We also note that the model of (3) is often bifurcated into "near-field" and "far-field" cases (Feuerstein, Blackard, Rappaport, Seidel, and Xia, 1994). Within the near-field, which is defined as within the first Fresnel zone, the model of (3) is an approximation with a relatively low path loss exponent. Beyond the first Fresnel zone, there tends to be more significant destructive multipath interference and the effective path loss exponent increases. As a result, more complete path loss vs. distance models are called "piecewise linear" path loss models and include two (or possibly more) $E[L_{ij}]$ log-linear functions of (3) for use with different ranges of $d_{ij}$. Within RSS-based localization systems, a piecewise linear path loss model requires more parameters to be estimated, but could provide more accurate localization, in particular from very short-range or very long-range RSS measurements. For WSN with sometimes high densities, sensors can often be in each others' near-field.

## Noise: Frequency-Selective Fading and Shadowing

Clearly, the measured path loss has other contributions which are not a function of distance. If measured path loss $\hat{L}_{ij} = E[L_{ij}]$ at all times on all links, we would have no problem estimating distance and we would be able to calculate it exactly. The measured $\hat{L}_{ij}$ suffers from fading and shadowing, which are commonly lumped together and called "fading error" or "noise". These errors are severe, much more significant than the 1 dB standard deviations of measurement or characterization error which we've been discussing so far. We refer to fading error on the link between i and j as $Y_{ij}$, and the shadowing loss on the link as $X_{ij}$. Then,

$$\hat{L}_{ij} = E[L_{ij}] + X_{ij} + Y_{ij} \quad (4)$$

where $E[L_{ij}]$ is given in Equation (3).

There are several key points about the model in (4) that allow us to analyze RSS-based localization.

- The shadowing loss $X_{ij}$ can be well approximated as Gaussian, since it is expressed in dB (Rappaport, 1996). Shadowing losses in linear terms are multiplicative, but in dB are additive. Thus, by a central limit theorem argument, the dB total loss after interaction with multiple attenuators can be considered to be Gaussian. In linear terms, this distribution is called log-normal.
- Fading errors are due predominantly to frequency-selective fading. The arriving multipath components add together, each with a phase and amplitude, and a phase that is a function of the frequency. At some frequencies, the phases are opposite and cancel, and we experience a "frequency null". At other frequencies, the phases are such that amplitudes add constructively. At one frequency, the fading error $Y_{ij}$ has a non-Gaussian distribution such as a Raleigh or Ricean (when loss expressed in linear terms).

We note that frequency selective fading can be reduced by performing wideband measurements. With narrowband radios, this translates into frequency hopping in order to make measurements at multiple different frequencies. When these frequencies are separated by more than the correlation bandwidth of the channel, we can expect the experienced fading losses to be uncorrelated (Rappaport, 1996). For example, both Mica2 and 802.15.4-compatible radios can be designed to switch frequencies. We suggest operating a slow frequency hopping protocol when using narrowband radios, in which sensors measure RSSI with their neighbors sequentially across a list of different frequencies. In our implementation (Patwari and Agrawal, 2006), we hop over 16 frequencies over the range of 900-928 MHz, and nodes save only an averaged path loss measurement. We find significant improvement in measured path loss when averaging, compared to without averaging. In general, for the average of N uncorrelated frequency measurements, we expect the standard deviation of $Y_{ij}$ to reduce by a factor of $\sqrt{N}$. Note that this average does little to reduce the variance of $X_{ij}$; small percentage frequency changes do not significantly change the attenuation experienced due to obstructions.

The distribution of $L_{ij}$, due to these two contributions, has both similarities and differences from the Gaussian distribution. Although $X_{ij}$ is approximately Gaussian, $Y_{ij}$ may or may not be Gaussian. When averaging over many different frequencies, it can be argued that $Y_{ij}$ will also be approximately Gaussian as well by another central limit argument. However, a Ricean or Rayleigh random variable converted to dB units will have noticeably heavier tails than the Gaussian distribution.

We can quantify from experiments how well the Gaussian assumption holds. For example, measurements of RSS from (Patwari, Wang, and O'Dea 2002) are used to test the Gaussian assumption in Figure 9. These measurements were of path loss in a narrow-band channel, and did not do any frequency averaging. First, we computed the fading error by subtracting $\bar{L}_{ij}$ from the path loss measurements $L_{ij}$. This fading error is then compared to the a unit-variance Gaussian distribution in a quantile-quantile plot, shown in Figure 9. If the data were exactly Gaussian, the data points would lie in a diagonal line. Within the -2 to +2 quantiles, the data lie very close to a Gaussian distribution. But, the extreme values of the measured fading errors show heavier tails, indicating the non-Gaussian nature of fading errors.

Another measurement set reported in (Patwari, Hero, Perkins, Correal, and O'Dea, 2003) showed similar results for RSS fading errors. In fact, it was reported that the RSS modeling error could be more accurately described as a Gaussian mixture, that is, one in which a large majority of data is described as Gaussian with one (smaller) variance, and a small fraction of the data is described as Gaussian with a different (larger) variance. Such a mixture distribution would explain the heavier tails seen in RSS fading errors. The work of Whitehouse, Karlof, Woo, Jiang, and Culler (2005), advocate using empirical cumulative distribution functions (CDFs) of measurement data directly as the distribution of

*Figure 9. Fading and shadowing losses on RSS measurements reported in (Patwari, Wang, and O'Dea, 2002) compared to a zero-mean, unit variance Gaussian distribution in a quantile-quantile plot. Data shows agreement between -2 to +2 quantiles, but somewhat heavier tails.*

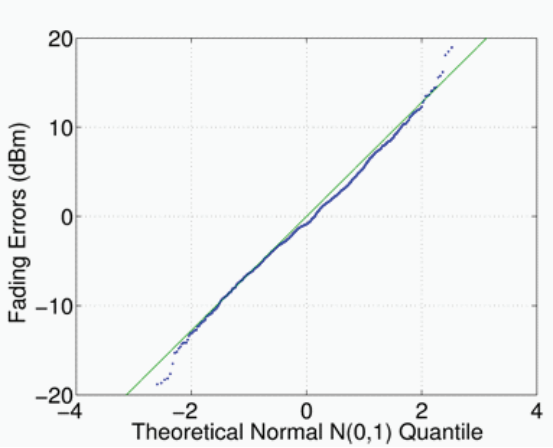


fading errors. Such CDFs could improve the accuracy of studies which use simulation to quantify the performance of RSS localization.

Mixture and empirical heavy-tailed distributions are analytically more difficult to deal with, but they motivate "robust estimation" of localization. Robust estimators down-weight or eliminate data points which seem inconsistent with other data. One example is to eliminate triplets of ranges which do not meet the triangle inequality, or distances among four nodes which do not meet the "robust quadrilateral" requirement (Moore, Leonard, Rus, and Teller, 2004). Such algorithms can eliminate some of the worst distance estimates.

We also note that in simulation, that shadowing errors experienced on different links (i,j) are taken to be independent and identically distributed, even though this is not a realistic assumption (Patwari, Wang, and O'Dea, 2002). In real life, the shadowing on different links may be correlated if the links are shadowed by the same obstructions. For example, two links passing through the same concrete wall would experience similar shadowing. In general, two links which cover similar ground may experience correlated shadowing (Agrawal and Patwari, 2008).

## Parameter Estimation

While we know that fading and shadowing will cause range errors when using a general path loss model such as (3), we also must have an accurate estimate for the parameters of the model in order to estimate distance. For (3), there are two parameters, $L_0$ and $n_p$, which are functions of the environment of deployment. One main difficulty in range estimation is determining these two parameters. In our implementations, we conduct measurements in the environment of interest, which allow us to estimate these parameters. This is a significant task. Current research is evaluating algorithms to adaptively estimate the two parameters, which would be a huge benefit to quick deployment of RSS-based localization systems, and would be essential for mobile sensor networks which may periodically change environment. One such adaptive approach is presented in (Li, 2006), which simultaneously estimates coordinates and the path loss exponent.

Without adaptive parameter estimation, we can, and often do, perform deployment experiments to determine path loss parameters. Typically, we would perform one deployment experiment in the environment of interest, which would then allow us to estimate the values of $L_0$ and $n_p$.

We must be aware that such experiments will also result in parameter estimates which are noisy. In order to demonstrate the variation in channel parameter estimates, we perform 15 deployment experiments in one single area, only changing the arrangement of the objects in that area between experiments. In this series of experiments, we arrange 16 Mica2 nodes on the floor in an empty classroom in an Engineering building on the University of Utah campus, after first removing all existing furniture from the room. The nodes are placed in a four by four grid, with grid points each four feet (1.2 meters). We generate a "random" arrangement of objects for each experiment by placing obstructions as dictated by a randomized Matlab script. For ease of use, our obstructions are ten cardboard boxes wrapped in aluminum foil. These are significant RF reflectors, if not attenuators. Since each experiment ran with identical quantity and quality of objects in the environment, we would intuitively expect the path loss model parameters to be identical.

During each experiment, we capture path loss integers, averaged over 16 frequencies (to which sensors hop during a slow frequency hopping protocol). In this experiment, all sensors use the same known transmit power code. Since we know the actual coordinates, we can plot the measured RSSI vs. actual distance. Then, we use linear regression to find the best linear fit between RSSI and distance. These linear fits are plotted in Figure 10. Finally, over all 15 experiments, we find the average linear fit, which is also plotted in Figure 10. We could have equivalently plotted a linear fit with path loss in dB using the known transmit power, reported battery voltages, and receiver characteristics of the nodes involved in the measurements, but have chosen to plot the direct RSSI measurement for simplicity.

## Discussion

At short range, there can be significant variations in the estimated path loss parameters – at 1 meter (0 dB meters), the standard deviation in RSSI is 4, which corresponds to approximately 1 dB. At longer distances, the standard deviation is in the range of 0.01 to 0.02 V RSSI, or 0.5 to 1 dB path loss. Al-

*Figure 10. Linear proportionality estimated in 15 deployment experiments between log of distance and RSSI value, and the average proportionality over all experiments*

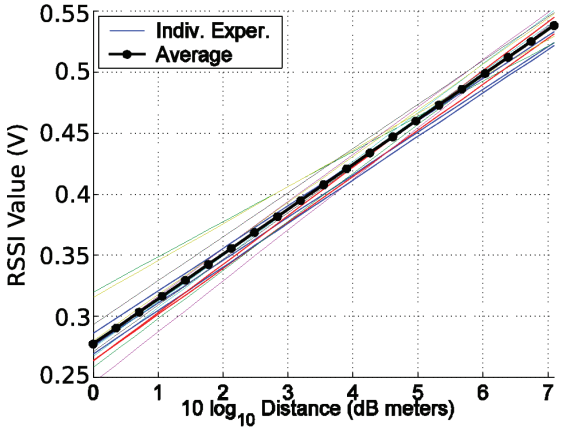

though these numbers are not severe, it is possible that the particular environment measured is not going to characterize that environment for all time. We would recommend that more than one deployment experiment be performed in order to robustly characterize an environment. In general, as we mentioned at the start of the "Parameter Estimation" section, it may be critical for large-scale deployments to use an algorithm which estimates model parameters and coordinates simultaneously, so that the specific environment in which deployed sensors is modeled appropriately.

## Distance Estimation Equations

Assuming that path loss parameters have been estimated for the environment of interest, we can estimate distance from path loss. Solving (4) for $d_{ij}$,

$$\hat{d}_{ij} = d_0 10^{(L_{ij} - L_0)/(10 n_p)} \tag{5}$$

As it turns out, this equation for $\hat{d}_{ij}$ is also the maximum likelihood estimator (MLE) of distance given measured path loss $L_{ij}$ and measured parameters $L_0$ and $n_p$. This means that as the noise reduces towards zero (as fading errors lessen), this estimator is efficient, that is, its variance approaches the lower bound on the variance of an unbiased estimator. Clearly, the MLE has favorable features. However, the MLE is a biased estimator of distance in this case. As pointed out in Patwari, Hero, Perkins, Correal, and O'Dea (2003), given the discussed Gaussian distribution for $L_{ij}$,

$$E[\hat{d}_{ij}] = C d_{ij}, \quad \text{where} \quad C = \exp\left\{ \frac{1}{2} \left[ \frac{\sigma_{dB} \log 10}{10 n_p} \right]^2 \right\} \tag{6}$$

For typical channel parameters (Rappaport 1996), C is between 1.08 and 1.2, adding 8-20% bias to the range estimate. Motivated by (6), we might also estimate distance $d_{ij}$ as,

$$\hat{d}_{ij}(BR) = \frac{d_0}{C} 10^{(L_{ij} - L_0)/(10 n_p)} \tag{7}$$

in order to remove the bias in the distance estimate. We denote this "bias-removed" estimator as $\hat{d}_{ij}(BR)$. The choice between (5) and (7) is left to the system designer – it is often the case that the localization algorithm introduces other biases, which may counteract the bias in Equation (5). However, if it does not, the use of (7) may reduce the localization errors in the algorithm.

Moreover, it is critical to note that when using RSS-based range estimates, the nodes separated by the shortest distances are going to produce the most accurate range estimates. Equivalently, longer distances will measure distance estimates which have higher variance. Intuitively, we can see that at longer range, the same error in measured RSSI will correspond to a larger distance error. For example, consider Figure 10. The conversion between RSSI and log distance is linear, but if log distance is high, then a change in log distance results in more linear distance change than at a low log distance. From another perspective, we can look at the variance of the MLE estimate of distance from (5),

$$\mathrm{Var}[\hat{d}_{ij}] = (C^4 - C) d_{ij}^2 \tag{8}$$

This shows that the standard deviation of the distance estimate is directly proportional to the actual distance. For example, if C = 1.15 and the actual distance is 1 meter, using (6) we would observe a standard deviation of the MLE range estimate of 0.77 meters -- but for an actual distance of 10 meters, we would expect a standard deviation of 7.7 meters. Clearly while 77 cm error may be acceptable, a range error of 7.7 meters would be very severe.

A good localization algorithm would use this relationship to strongly down-weight range estimates to distant neighbors and instead emphasize range estimates between nearby neighbors. Further, it quantifies the notion that RSS will be most accurate at short range, as we expect from the discussion in the "Propagation Effects" section.

## DISCUSSION

There are clearly many issues that negatively impact RSS-based localization, and it is easy to criticize or neglect the capabilities of RSS in localization without considering its capabilities and successes. In terms of commercial application, we have mentioned deployments of indoor localization systems using RF fingerprint-based algorithms, and there have also been successful commercial deployments by AwarePoint, Inc., which use a WSN-like mesh network of nodes and use distance-based algorithms to estimate node locations.

In terms of research literature, there have been a number of algorithms proposed and studied which consider the effects of ranging error and device inaccuracies. We have mentioned many such references in the text, and many good reviews of RSS-based localization algorithms exist in the literature, for example, Elnahraway, Li, and Pahlavan (2004).

This chapter is not intended to discuss the wide literature on localization algorithms, which may be the subject of many chapters of this book. Instead, we reiterate major lessons learned during device calibration and path loss model parameter estimation to recommend several simple adaptations which RSS-based location algorithms can take in order to improve their robustness and accuracy:

- Use of slow frequency hopping and averaging RSSI over frequency to reduce frequency-selective fading effects,
- Use of transmit power control to avoid the two opposite extreme problems of RSSI saturation and lack of connectivity,
- If transmit powers are known to have high variation, do not average bi-directional path losses $L_{ij}$ and $L_{ji}$ and instead use their differences to estimate the transmit power of each node.
- Down-weighting of the range estimates to the furthest neighbors (or equivalently emphasis given to nearest neighbors' range estimates),
- Adaptive estimation or learning of path loss parameters in the local environment of the deployment when using distance-based algorithms,
- Non-parametric approaches which compare signal strength measurements to each other, rather than to estimate distances directly.

For each of these bullet points, some existing literature has been discussed in this chapter. Future research in algorithms will be critical to achieve the best possible RSS-based localization performance without large deployment expense. Researchers and developers with experience in the measurement

and calibration of received signal strength will be best able to understand the interactions between real-world measurements of RSS and localization algorithms.

## CONCLUSION

While signal strength may be a highly desirable measurement for sensor self-localization algorithms, it is not necessarily straight-forward to obtain measurements which can be used to estimate sensor location to the best degree possible. We have presented a calibration procedure which can be used with any wireless sensor, and shown the results of one such set of calibration experiments. Critically, deployed sensor location systems must localize based on path loss rather than RSSI or received power, since the transmit power of sensors may vary. We have motivated key location system adaptations which may be used to reduce measurement and thus localization errors, for example, transmit power control to reduce the problem of RSSI saturation; and frequency hopping to reduce multipath fading error. We discuss both distance-based estimation and range-free estimation, in particular adaptations which eliminate modeling requirements or transmit power variation effects. Using these methods, we can maximize the ability of signal strength measurements to provide accurate inputs into localization algorithms, such as those described within this book.

## ACKNOWLEDGMENT

This material is based in part upon work supported by the National Science Foundation under CAREER grant ECCS-0748206 and CyberTrust grant CNS-0831490. Any opinions, findings, and conclusions or recommendations expressed in this material are those of the author(s) and do not necessarily reflect the views of the National Science Foundation.

## REFERENCES

Agrawal, P., & Patwari, N. (2008). *Correlated Link Shadow Fading in Multi-hop Wireless Networks*, (Tech Report arXiv:0804.2708v2), arXiv.org. Retrieved 18 Apr 2008 from http://arxiv.org/abs/ 0804.2708v2

Bahl, P., & Padmanabhan, V. N. (2000). RADAR: An In-Building RF-Based User Location and Tracking System. *In Proc. 19th International Conference on Computer Communications (Infocom)*, 2, 775–784.

Bulusu, N., Heidemann, J., & Estrin, D. (2000). GPS-less low-cost outdoor localization for very small devices. *IEEE Personal Communications, 7*(5), 28-34.

Costa, J., Patwari, N., & Hero, A. O. (2006). Distributed weighted-multidimensional scaling for node localization in sensor networks. *ACM Trans. Sensor Networks, 2*(1), 39-64.

Durgin, G., Rappaport, T. S., & Xu, H. (1998). Measurements and models for radio path loss and penetration loss in and around homes and trees at 5.85 GHz. *IEEE Trans. Communications, 46*(11), 1484-1496.

Elnahraway, E., Li, X., & Martin, R. P. (2004). The limits of localization using RSS. *In Proceedings of the 2nd Intl. Conf. on Embedded Networked Sensor Systems* (pp. 283-284), Baltimore, MD.

Fang, S.-H., Lin, T.-N., & Lin, P.-C. (2008), Location Fingerprinting In A Decorrelated Space. *IEEE Trans. Knowledge and Data Engineering, 20*(5), 685-691.

Feuerstein, M. J., Blackard, K. L., Rappaport, T. S., Seidel, S. Y., & Xia, H. H. (1994). Path loss, delay spread, and outage models as functions of antenna height for microcellular system design. *IEEE Trans. Vehicular Technology, 43*(3), 487-498.

Hashemi, H. (1993). The indoor radio propagation channel. *Proc. IEEE, 81*(7), 943–968.

He, T., Huang, C., Blum, B. M., Stankovic, J. A., & Abdelzaher, T. (2003). Range-free localization schemes for large scale sensor networks. *In Proc. 9th Intl. Conf. on Mobile Computing and Networking (Mobicom'03)*, (pp. 81-95), San Diego, CA.

King, T., Kopf, S., Haenselmann, T., Lubberger, C., & Effelsberg, C. W. (2006). COMPASS: A Probabilistic Indoor Positioning System Based on 802.11 and Digital Compasses. *In Proc. 1st ACM Intl. Workshop on Wireless Network Testbeds, Experimental Evaluation & Characterization (WiNTECH)*, (pp. 34-40), Los Angeles, USA.

Krishnamachari, B. (2006). *Networking Wireless Sensors*.Cambridge University Press.

Li, X. (2006). RSS-Based Location Estimation with Unknown Pathloss Model. *IEEE Trans. Wireless Communications, 5*(12), 3626-3633.

Liu, C., Wu, K., & He, T. (2004). Sensor localization with ring overlapping based on comparison of received signal strength indicator. *In Proc. IEEE Mobile Ad-hoc and Sensor Systems (MASS)*, (pp. 516–518).

Moore, D., Leonard, J., Rus, D., & Teller, S. (2004). Robust distributed network localization with noisy range measurements. *In Proc. 2nd Intl Conf. Embedded Networked Sensor Systems*, (pp. 50-61), Baltimore, MD.

Niculescu, D., & Nath, B. (2001). Ad Hoc Positioning System (APS). *In Proc. IEEE Global Communications Conference (GLOBECOM '01), 3*, 1734- 1743.

Pahlavan, K., Li, X., & Makela, J. P. (2002) Indoor geolocation science and technology. *IEEE Communications Magazine, 40*(2), 112-118.

Patwari, N., Wang, Y., & O'Dea, R. J. (2002). The Importance of the Multipoint-to-Multipoint Indoor Radio Channel in Ad Hoc Networks. *In Proceedings of the IEEE Wireless Communication and Networking Conference (WCNC'02), 2*, 608-612, Orlando FL.

Patwari, N., Hero, A. O., Perkins, M., Correal, N. S., & O'Dea, R. J. (2003). Relative Location Estimation in Wireless Sensor Networks. *IEEE Trans. Signal Processing, 51*(8), 2137-2148.

Patwari, N., & Hero, A. O. (2003). Using proximity and quantized RSS for sensor localization in wireless networks. *In Proc. 2nd ACM Intl. Conf. Wireless Sensor Networks and Applications (WSNA '03)* (pp. 20-29), San Diego, CA.

Patwari, N., Agrawal, P., & Hero, A. O. (2006). Demonstrating Distributed Signal Strength Location Estimation. *In Proc. Fourth Intl. Conf. Embedded Networked Sensor Systems (SenSys'06)*, (pp. 353-354), Boulder, CO.

Patwari, N., & Hero, A.O. (2006). Signal strength localization bounds in ad hoc & sensor networks when transmit powers are random. *In Proceedings of the Fourth IEEE Workshop on Sensor Array and Multichannel Processing* (SAM-2006) (pp. 299-303), July 12-14, 2006, Waltham, MA.

Rappaport, T. S. (1996). *Wireless Communications: Principles and Practice*. Englewood Cliffs, NJ: Prentice-Hall.

Whitehouse, K., Karlof, C., Woo, A., Jiang, F., & Culler, D. (2005). The effects of ranging noise on multihop localization: an empirical study. *In Proc. 4th Intl. Symp. Information Processing in Sensor Networks (IPSN'05)* (pp. 73-80), April 24 - 27, 2005 Los Angeles, California.

Whitehouse, K., Karlof, C., & Culler, D. (2007). A practical evaluation of radio signal strength for ranging-based localization. SIGMOBILE Mob. *Comput. Commun. Rev. 11*(1), 41-52.

Yedavalli, K., Krishnamachari, B., Ravula, S., & Srinivasan, B. (2005). Ecolocation: a sequence based technique for RF localization in wireless sensor networks. *In Proc. 4th Intl. Symp. Information Processing in Sensor Networks*, (pp. 285-292), Los Angeles, CA.

Zhu, J. (2006). *Indoor/Outdoor Location of Cellular Handsets Based on Received Signal Strength*. Doctoral dissertation, Georgia Tech, Atlanta. Retrieved Aug 12, 2008, from http:// etd.gatech.edu/theses/available/etd-05182006-154920/

Zuniga, M. Z., & Krishnamachari, B. (2007). An analysis of unreliability and asymmetry in low-power wireless links. *ACM Trans. Sensor Networks, 3*(2), 1-7.